SPACE-CHARGE OSCILLATIONS IN A SELF-MODULATED ELECTRON BEAM IN MULTI-UNDULATOR FREE-ELECTRON LASERS

J. Rosenzweig, C. Pellegrini, L. Serafini*, C. Ternienden and G. Travish

UCLA Dept. of Physics and Astronomy

405 Hilgard Ave., Los Angeles, CA 90095-1547

ABSTRACT

In this paper we examine the oscillation of electron-beam density perturbations (longitudinal plasma oscillations) produced at the exit of a high-gain free-electron laser (FEL) by the action of the FEL instability. These oscillations, which are analyzed in the case of both a free-space drift and a dispersive section, can degrade the bunching of the beam in the drift between undulator sections in multi-stage FELs. The impact of these oscillations on the gain of an FEL in an undulator following such a drift, as well as the case of an optical klystron is studied.

*Permanent address: INFN-Milano, Via Celoria 16, 20133 Milan, Italy.

Submitted to the Proceedings of the 1996 Advanced Accelerator Workshop

Lake Tahoe, October 12-18, 1996

I. LONGITUDINAL SPACE-CHARGE

In space-charge dominated beams derived from rf photoinjectors such as typically drive moderate energy (few tens of MeV) free-electron lasers (FELs), the collective transverse motion is characterized by single-component plasma behavior. The free expansion due to the repulsive self-forces is controlled by the externally imposed focusing lattice, producing beam envelope, or surface plasma oscillations. In contrast, for many beams, the longitudinal space charge forces do not produce significant debunching, and small efforts (running slightly off of rf crest) are necessary to compensate the energy slew introduced by the space-charge forces. This is because in the beam rest frame, the bunch length is much larger than the radius $\gamma_0\sigma_z >> \sigma_r$, and the longitudinal surface plasma oscillation frequency is much smaller than the transverse frequency. This can be quantified by a geometric correction factor for plasma frequencies based on the envelope approach due to Lapostolle[1]

$$\begin{aligned} \omega_{p\perp} &= \sqrt{\frac{2\pi e^2 n_b}{\gamma_0^3 m_e} f\left(\frac{\gamma_0\sigma_z}{\sigma_r}\right)} \\ \omega_{p\parallel} &= \sqrt{\frac{2\pi e^2 n_b}{\gamma_0^3 m_e}\left(1 - f\left(\frac{\gamma_0\sigma_z}{\sigma_r}\right)\right)} \end{aligned} \tag{1.1}$$

where we can approximate $f(x) \cong \left[\frac{x^2}{4+x^2}\right]^{1/4}$. It can be seen that under the condition that $\gamma_0\sigma_z >> \sigma_r$ that $f(x) \Rightarrow 1$, and the longitudinal plasma frequency approaches zero, $\omega_{p\parallel} \propto \sigma_r/\gamma_0\sigma_z$, as the field becomes nearly purely transverse, $E_z \propto (\sigma_r/\gamma_0\sigma_z)^2$. The physical basis of determining plasma oscillation frequencies will be illustrated further by the discussion below.

For short-wavelength longitudinal density perturbations (microbunching) such as are introduced by the FEL process, however, the field is no longer transverse, as the

longitudinal density gradients may have a rest frame scale length shorter than the beam width. In the ultra-short wavelength limit, the electric field associated with a periodic density perturbation

$$n_1 \equiv n_b - n_{b0} = \delta n_b \cos(k_r \zeta) \tag{1.2}$$

of wavelength $\lambda_r = 2\pi / k_r$, with n_{b0} the unperturbed beam density, and $\zeta = z - v_{b0} t$ (distance measured in the Galillean frame moving with the beam) is

$$E_{z1} \cong -\frac{4\pi e \delta n}{k_r} \sin(k_r \zeta). \tag{1.3}$$

For a constant density bunch distribution with a hard edge at radius a, the longitudinal electric field inside of the beam is given by

$$E_{z1} \equiv -\frac{4\pi e \delta n}{k_r} \sin(k_r \zeta) \left[1 - \frac{k_r a}{\gamma_0} K_0\left(\frac{k_r a}{\gamma_0}\right) I_0\left(\frac{k_r r}{\gamma_0}\right) \right]. \tag{1.4}$$

In the limit that the beam radius is large compared to the oscillation wavelength in the beam rest frame ($k_r a >> \gamma_0$), the correction factor in to Eq. 1.3 found in Eq. 1.4 approaches unity. In the case of the FEL the radiation wavenumber has a strong dependence on the normalized energy, $k_r \propto \gamma_0^2$, and so this situation, where the longitudinal space-charge force attains its one-dimensional limiting strength, is to be expected for any beam of moderate energy or above (*i.e.* the UCLA IR FEL $k_r \sigma_r \approx \gamma_0$, while for the TTF-FEL $k_r \sigma_r >> \gamma_0$). We shall therefore be concerned for the remainder of this work with one-dimensional plasma oscillations in FEL-microbunched beams. A detailed analysis of a the fields in two-dimensional microbunched beam, including higher harmonic bunching, is included in Appendix A.

II. LONGITUDINAL PLASMA OSCILLATIONS

We now derive the equations for small amplitude, linear, one-dimensional plasma oscillations in a microbunched beam. We consider the beam to be initially a cold plasma - a continuous, infinitely wide electron beam with average velocity v_{b0} and density n_{b0}. The effect of the FEL instability is, in addition to the density perturbation defined by Eq. 1.1, where $|n_1| << n_{b0}$ is required for linearity, a self-consistent small perturbation in the beam velocity

$$v_1 \equiv v_b - v_{b0}, \tag{2.1}$$

where we again require $|v_1| << v_{b0}$.

We begin the derivation of the longitudinal plasma oscillation equations by examining the equation of continuity in one-dimension

$$\frac{\partial \rho}{\partial t} + \vec{\nabla} \cdot \vec{J} = \frac{\partial \rho}{\partial t} + \frac{\partial J_z}{\partial z} = 0 \tag{2.2}$$

where beam charge density $\rho = -en_b$ and density $J_z = \rho v_b$ in the case of a cold fluid.

Keeping only terms linear in perturbed quantities in Eq. 2.1 we have

$$\frac{\partial n_1}{\partial t} + v_{b0} \frac{\partial n_1}{\partial z} + n_{b0} \frac{\partial v_1}{\partial z} = 0. \tag{2.3}$$

In order to relate the density and velocity to the electric field, we must use the momentum, defined relativistically as

$$p_z = p = \beta\gamma m_e c \equiv \frac{\beta}{\sqrt{1-\beta^2}} m_e c \tag{2.4}$$

This relation allows us to write the relationship between the differential (in that they are perturbed quantities) velocity v_1 and momentum p_1

$$\frac{p_1}{p_0} = \gamma_0^2 \frac{v_1}{v_{b0}}. \tag{2.5}$$

The rate of change in momentum of a fluid electron due to an electric field is therefore

$$\frac{dp_1}{dt} = m_e \gamma_0^3 \frac{dv_1}{dt} = -eE_{z1}. \tag{2.6}$$

This equation is valid for the perturbed system only - in a non-neutral plasma such as an electron beam, there is a zeroth order expansion of the beam, as discussed above, which is governed by the zeroth order electric field. As we are only interested in the oscillations affecting the microbunching, our treatment neglects this generally small effect.

It is instructive in this context to write the total time derivative of a fluid quantity in terms of its partial and convective components,

$$\frac{d}{dt} = \frac{\partial}{\partial t} + v_{b0} \frac{\partial}{\partial z}, \tag{2.7}$$

which allows us to recast Eq. 2.6 as

$$\left(\frac{\partial}{\partial t} + v_{b0} \frac{\partial}{\partial z}\right) v_1 = -\frac{e}{m_e \gamma_0^3} E_{z1}. \tag{2.8}$$

Differentiating Eq. 2.2 once with respect to time and using Eq. 2.8 we now have

$$\left(\frac{\partial}{\partial t}+v_{b0}\frac{\partial}{\partial z}\right)^2 n_1=\frac{en_{b0}}{m_e\gamma_0^3}\frac{\partial E_{z1}}{\partial z}. \tag{2.9}$$

We can now write the equation for plasma oscillations using the divergence of the electric field,

$$\vec{\nabla}\cdot\vec{E}=\frac{\partial E_z}{\partial z}=-4\pi e n_1, \tag{2.10}$$

to obtain a relation containing only the perturbed density,

$$\left(\frac{\partial}{\partial t}+v_{b0}\frac{\partial}{\partial z}\right)^2 n_1+\omega_p^2 n_1=\frac{d^2}{dt^2}n_1+\omega_p^2 n_1=0 \tag{2.11}$$

where

$$\omega_p^2=\frac{4\pi e^2 n_{b0}}{\gamma_0^3 m_e} \tag{2.12}$$

defines the microbunching plasma frequency. The factor of $\sqrt{2}$ difference in the plasma frequencies defined by Eq. 1.1 and Eq. 2.12 arises from the fact that the former describes surface plasma oscillations, while the latter is appropriate for internal, bulk plasma oscillations.

If we now use the distance down the beamline as the independent variable, we can formulate Eq. 2.11 as

$$\frac{d^2}{dz^2}n_1+k_p^2 n_1=0, \tag{2.13}$$

with $k_p^2 = \omega_p^2 / v_{b0}^2 = 4\pi r_e n_{b0} / \beta_0^2 \gamma_0^3$. It should be noted that Eq. 2.13 does not contain derivatives with respect to the spatial variable $\zeta = z - v_{b0} t$, and so a small amplitude disturbance in the beam density is stationary in the rest frame position - each beam "slice" is an independent oscillator. This is always the case for electrostatic plasma oscillations in a cold, uniform ambient density plasma.

The general solution for a density oscillation described by Eq. 2.13 is

$$n_1(z,\zeta) = n_1(0,\zeta)\cos(k_p z) + \frac{n_1'(0,\zeta)}{k_p}\sin(k_p z), \tag{2.14}$$

where the prime indicates a derivative with respect to z. It would appear that there are two constants associated with this solution, but in fact the equation of continuity (Eq. 2.3) relates them by

$$n_1(0,\zeta) = \frac{1}{v_{b0}}\frac{dn_1}{dt} = -\frac{n_{b0}}{v_{b0}}\frac{\partial v_1}{\partial z}\bigg|_{z=0} = -\frac{n_{b0}}{v_{b0}}\frac{\partial v_1}{\partial \zeta}\bigg|_{z=0}. \tag{2.15}$$

III. LONGITUDINAL DYNAMICS IN BETWEEN FEL UNDULATOR SECTIONS

In order to use Eqs. 2.14-15 to analyze the longitudinal plasma oscillations occuring after an undulator section, we must have a model for the microbunching which occurs in the undulator. We have, from the theory of the SASE FEL process,

$$\frac{p_1}{p_0} = \gamma_0^2 \frac{v_1}{v_{b0}} = \rho_{FEL} b_1 \cos(k_r \zeta) \tag{3.1}$$

where $b_1 = \delta n_b / n_{b0}$ is the bunching factor, or fractional modulation of the beam due to the action of the ponderomotive potential, which has a periodicity very close to the radiation

wavelength $2\pi/k_r$. Here, also $\rho_{\mathrm{FEL}} = \left[\frac{a_w k_p}{4k_w}\right]^{2/3}$ is the FEL[2] or Pierce parameter, k_w is the wavenumber of the undulator field, and a_w is its normalized strength. The bunching in configuration space is one-quarter of a wavelength out of phase with that in velocity space,

$$n_1(0,\zeta) = n_{b0} b_1 \sin(k_r \zeta) \tag{3.2}$$

Combining Eqs. 3.1 and 2.15, we have

$$\frac{v_1}{v_{b0}} = \frac{\rho_{\mathrm{FEL}} b_1}{\gamma_0^2} \cos(k_r \zeta), \tag{3.3}$$

and

$$n_1'(0,\zeta) = n_{b0} k_r \frac{\rho_{\mathrm{FEL}} b_1}{\gamma_0^2} \sin(k_r \zeta). \tag{3.4}$$

The plasma oscillations described by Eq. 2.14 are given, in the case of the SASE FEL bunched beam, by

$$n_1(z,\zeta) = b_1 n_{b0} \sin(k_r \zeta)\left[\cos(k_p z) + \frac{k_r}{k_p}\frac{\rho_{\mathrm{FEL}}}{\gamma_0^2}\sin(k_p z)\right]. \tag{3.5}$$

This expression shows that the bunching is enhanced for propagation distances less than one-quarter of a plasma wavelength. The maximum in the beam density occurs within this distance, and is given by

$$n_{1,\max} = b_1 n_0 \sqrt{1 + \left(\frac{k_r}{k_p} \frac{\rho_{\mathrm{FEL}}}{\gamma_0^2} \right)^2} \,. \tag{3.6}$$

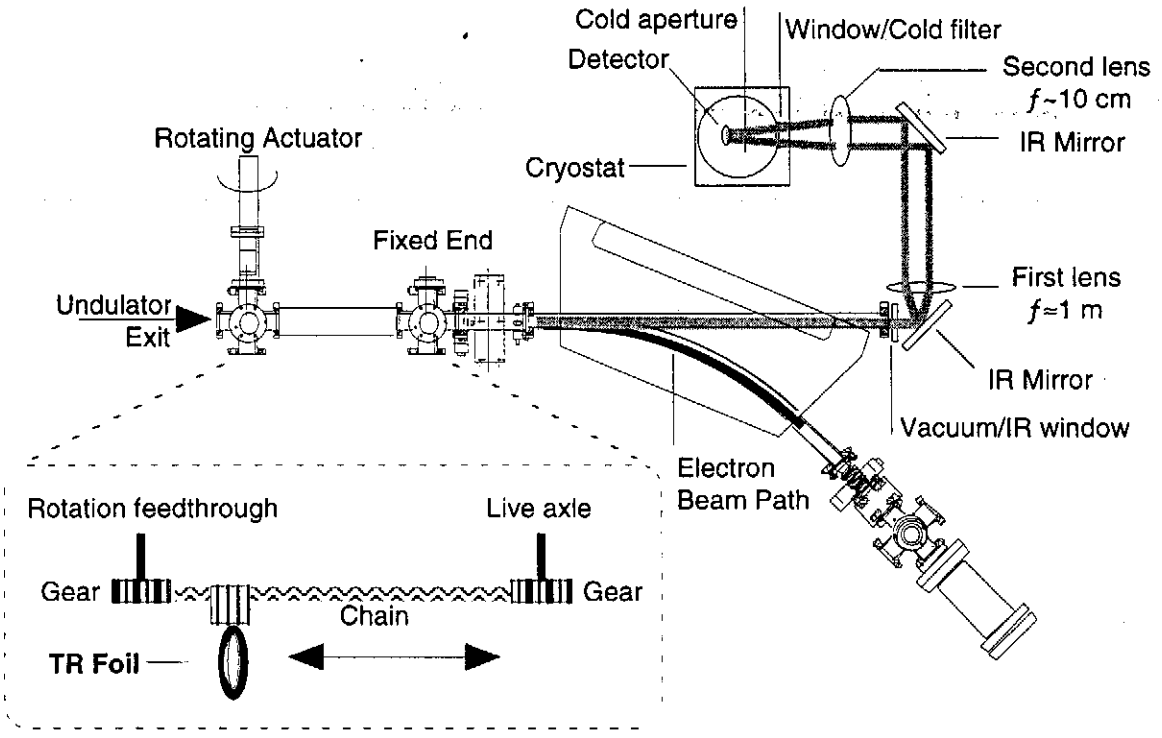

Figure 1. Experimental setup for CTR measurement of space-charge oscillations in FEL-induced beam microbunching.

The squared term in Eq. 3.6 represents the additional bunching due to the initial velocity distribution at the end of the undulator. In the limit of a beam with negligibly small space-charge, this number is much larger than unity, which corresponds to the tight bunching one expects from a velocity modulated beam with no repulsive self-force active. It should also be noted that this extra bunching term is proportional to $\rho_{FEL}^{-1/2}$, with no explict dependence on the beam energy. This term is less than unity for beams with high gain, typically in the Raman regime. For the UCLA IR FEL case[3] this number is approximately 2.3, and so the beam bunches more tightly by an additional factor of 150%.

This occurs very quickly after the undulator, because in this case $k_p^{-1} = 21$ cm, with the maximum beam density at $z \equiv 3\pi/8k_p = 25$ cm. The oscillation proceeds towards smaller bunching after this point, with the null occuring at $z = 7\pi/8k_p = 30.2$ cm. After the null, the bunching reverses (to the extent that the assumption of one-dimensional laminar flow holds), at maximizes again after an additional one-quarter plasma period. We plan to investigate these phenomena at the UCLA IR FEL using the coherent transition radiation-based microbunching diagnostic we have developed, with the transition radiator placed at a number of positions downstream of the undulator[4]. The experimental setup for this measurement is shown in Fig. 1.

For the TTF-FEL in its initial stage[5], we take for the sake of example the energy as 500 MeV, the rms bunch length beam $\sigma_z = 50$ μm, and the rms beam size $\sigma_r = 50$ μm. In this case, we have $k_p^{-1} = 300$ cm, which is a relatively short length considering the energy of the beam. The additional bunching factor for these TTF-FEL parameters is $\frac{k_r}{k_p}\frac{\rho_{\mathrm{FEL}}}{\gamma_0^2} = 4.5$ (twice that of the UCLA case, as ρ_{FEL} is four times smaller), and the bunching factor increases in a inter-undulator module drift by approximately this factor if the drift length is chosen to be approximately $z = 3\pi/7k_p = 400$ cm. One is likely to have shorter drifts in practice, which produce smaller density enhancements. One possible way to circumvent this is to use an optical klystron configuration, in which a short dispersive section allows enhanced pulse compression in a shorter propagation distance.

IV. Space-Charge Oscillations in Dispersive Sections: the Optical Klystron

The use of a dispersive section at the end of an FEL undulator serves to enhance the phase bunching of the electron distribution by introducing a change in the relationship between the longitudinal velocity and the momentum,

$$\frac{v_1}{v_{b0}} = \frac{p_1}{p_0}\left(\frac{1}{\gamma_0^2} - \frac{\eta_x}{R}\right). \tag{4.1}$$

For high energy electrons, the second, dispersive path-length term on the right side of Eq. 4.1 is dominant in cases of interest. A chicane, which is basically one period of a long wavelength undulator, is typically used to give an average horizontal dispersion which is negative, and so the bunching proceeds in the same direction as pure velocity bunching.

The introduction of this additional effect changes the plasma oscillation equation 2.11 (and expressions derived from it), by a redefinition of the plasma frequency,

$$\omega_{p,ch}^2(z) = \frac{4\pi e^2 n_{b0}}{\gamma_0 m_e}\left(\frac{1}{\gamma_0^2} - \frac{\eta_x(z)}{R}\right) \cong \frac{4\pi e^2 n_{b0}}{\gamma_0 m_e}\left(\frac{-\eta_x(z)}{R}\right). \tag{4.2}$$

This frequency has an explicit dependence on z, which makes the oscillation equation not easily integrable. If we average the dispersion over the chicane section, we can assign an average value to it in Eq. 4.2,

$$\left\langle -\frac{\eta_x}{R}\right\rangle \equiv \frac{a_{ch}^2}{2\gamma_0^2} \equiv \frac{\theta^2}{2}, \tag{4.3}$$

where $a_{ch} >> 1$ is the equivalent undulator parameter, and θ is the maximum bend angle in the chicane section.

Taking this average value of the dispersion, we can again integrate the oscillation equations to obtain the equivalent of Eq. 3.5,

$$n_1(z,\zeta) = b_1 n_{b0} \sin(k_r\zeta)\left[\cos(k_{p,ch}z) + \frac{k_r}{k_{p,ch}}\frac{a_{ch}^2\rho_{FEL}}{2\gamma_0^2}\sin(k_{p,ch}z)\right], \tag{4.4}$$

where $k_{p,ch} = \omega_{p,ch} / v_{b0}$. The maximum enhancement of the bunching is now approximately larger, by a factor of $a_{ch} / \sqrt{2}$ from the case of a pure drift. This is the same factor by which the plasma frequency is raised.

Because the plasma oscillation wavelength $2\pi / k_{p,ch}$ is shortened, in the case of the UCLA IR FEL it may be difficult to attempt chicane bunching after the initial 60 cm undulator section. For the TTF-FEL example, however, there may be much to be gained by employing a chicane section in the so-called optical klystron mode[6]. Assuming a chicane section 66 cm long, which with $a_w = 10$ corresponds to one-quarter of a plasma oscillation length, the bunching enhancement is then raised to approximately 31 at the exit of the chicane.

V. FUTURE WORK

It is interesting to note that the results obtained above are independent of microbunching amplitude as long as $|n_1| << n_{b0}$, i.e. the wave is of small amplitude. For inter-undulator sections of a multi-undulator array in an FEL amplifier, this condition is not violated, as saturation ($|n_1| \approx n_{b0}$) is only exponentially approached in the final undulator section. Even so, it the results of this paper can be extended to include large amplitude oscillations in a straightforward way. It is well known that the density profile of a large amplitude one-dimensional plasma wave can be expanded in a power series of Fourier amplitudes[7]. The harmonics in the density wave associated with the large amplitude dynamics can then be analyzed separately. The two-dimensional corrections to the nominally longitudinal field, including the effects of these higher harmonics, are explored in Appendix A.

An integrated theory of the interplay between space-charge and FEL action, including undulators, drifts, and dispersive sections, based on the linearized SASE theory of Bonifacio, Narducci and Pellegrini, is now under development. Preliminary numerical

results verify the conclusions based on the linearized fluid theory presented above. It is hoped that features of both the theoretical and computational approaches to this problem will be verified soon at the UCLA IR FEL experiment[3-4].

It should also be pointed out that the general subject of treatment of space-charge oscillations in relativistic beams in both drifts and chicanes occurs outside of the context of FELs. An example of current interest is the so-called plasma klystron[8], which has been proposed as an injector for ultra-short wavelength acceleration schemes such as the plasma beatwave accelerator.

REFERENCES

1. P. Lapostolle, *Proton Linear Accelerators* (Los Alamos National Laboratory, 1980). Also, the functional dependence of the electric fields on the beam rest frame aspect ratio has been explored in the work by L. Serafini, "Microbunch production with rf photoinjectors", *IEEE Trans. on Plasma Science,* **24**, 1 (1996).

2. R. Bonifacio, C. Pellegrini and L. Narducci. *Opt. Commun.* **50,** 313 (1984).

3. G. Travish, M. Hogan, C. Pellegrini, and J. Rosenzweig, "The UCLA high gain infrared FEL" *Nucl. Instr. Methods A* **358**, ABS 75 (1995).

4. J. Rosenzweig, G. Travish and A. Tremaine, "Coherent transition radiation diagnosis of electron beam microbunching", *Nucl. Instr. Methods A.* **365,** 255 (1995).

5. J. Rossbach, *et al.*, "Conceptual Design Report of the TESLA-FEL", in preparation.

6. J.C. Gallardo and C. Pellegrini, "Optical klystron configuration for a high gain X-ray free-electron laser", *Opt. Commun.* **77,** 45 (1990).

7. J.B. Rosenzweig, "Trapping, thermal effects, and wave breaking in the nonlinear plasma wake-field accelerator", *Phys. Rev. A* **38,** 3634 (1989).

8. T. Katsouleas, *et al.* "A plasma klystron for generating ultra-short electron bunches", *IEEE Trans. on Plasma Science,* **24**, (1996).

APPENDIX A: CALCULATION OF THE SPACE CHARGE ELECTRIC FIELD

We begin with a general, radially uniform (to a hard edge) charge distribution bunched at many harmonics, moving relativistically in the z-direction, which is written in the laboratory frame as

$$\rho = \rho_0\left(1+\sum_{h=1}^{\infty} b_h \cos\phi_h\right), \tag{A.1}$$

where $\rho_0 = -en_{b0}$ the phase dependence of each harmonic is given by $\phi_h = hk\zeta + \theta_h$, $\lambda = 2\pi/k$ being the fundamental periodicity of the distribution. We transform the space charge density distribution given in Eq. A.1 into the beam rest frame (r,z'). In this rest frame the charge density ρ_{rest} now reads:

$$\rho_{rest} = \begin{cases} \dfrac{\rho_0}{\gamma_0}\left[1+\sum_{h=1}^{\infty} b_h \cos\left(h\dfrac{k}{\gamma_0}z'+\theta_h\right)\right] & 0 \le r \le a \\ 0 & r \ge a \end{cases}. \tag{A.2}$$

In order to calculate the electrostatic potential associated to this distribution (the problem is approximately electrostatic one in this reference frame), we split the density ρ_{rest} into two terms, one (trivial) corresponding to the constant density, and the second (of interest) representing the oscillating components

$$\rho_{rest} = \begin{cases} \dfrac{\rho_0}{\gamma}\sum_{h=1}^{\infty} b_h \cos\left(h\dfrac{k}{\gamma}z'+\theta_h\right) & 0 \le r \le a \\ 0 & r \ge a \end{cases} \tag{A.3}$$

Let us consider the Poisson equation $\nabla^2\varphi_h(r,z') = -4\pi\rho_{rest,h}(r,z')$ for the h-th component, where $\rho_{rest,h}(r,z') = \dfrac{\rho_0 b_h}{\gamma}\cos\left(h\dfrac{kz'}{\gamma}+\theta_h\right)$. To solve this equation we

factorize the dependence of the potential function $\varphi_h(r,z')$ on the two cylindrical co-ordinates r and z': $\varphi_h(r,z') = f(z')g(r)$; $0 \le r \le a$ and $\varphi_h(r,z') = \sigma(z')\tau(r)$; $r \ge a$. Poisson equation becomes:

$$\begin{cases} \dfrac{1}{g(r)}\dfrac{d^2g(r)}{dr^2} + \dfrac{1}{rg(r)}\dfrac{dg(r)}{dr} + \dfrac{1}{f(z')}\dfrac{d^2f(z')}{dz'^2} = -\dfrac{4\pi\rho_0 b_h}{\gamma}\dfrac{\cos\left(h\dfrac{k}{\gamma}z' + \theta_h\right)}{f(z')g(r)} & ; \ 0 \le r \le a \\ \dfrac{1}{\tau(r)}\dfrac{d^2\tau(r)}{dr^2} + \dfrac{1}{r\tau(r)}\dfrac{d\tau(r)}{dr} + \dfrac{1}{\sigma(z')}\dfrac{d^2\sigma(z')}{dz'^2} = 0 & ; \quad r \ge a \end{cases} \tag{A.4}$$

Setting $f(z') = A\dfrac{4\pi\rho_0 b_h}{\gamma}\cos\left(h\dfrac{k}{\gamma}z' + \theta_h\right)$ and $\sigma(z') = B\cos\left(h\dfrac{k}{\gamma}z' + \theta_h\right)$, the two equations are transformed into:

$$\begin{cases} r^2\dfrac{d^2g(r)}{dr^2} + r\dfrac{dg(r)}{dr} - \left(h\dfrac{k}{\gamma}r\right)^2 g(r) = -\dfrac{r^2}{A} & ; \ 0 \le r \le a \\ r^2\dfrac{d^2\tau(r)}{dr^2} + r\dfrac{d\tau(r)}{dr} - \left(h\dfrac{k}{\gamma}r\right)^2 \tau(r) = 0 & ; \quad r \ge a \end{cases} \tag{A.5}$$

and further into:

$$\begin{cases} x^2\dfrac{d^2g(x)}{dx^2} + x\dfrac{dg(x)}{dx} - x^2g(x) = -\dfrac{\gamma^2}{Ah^2k^2}x^2 & ; \ 0 \le x \le \dfrac{hka}{\gamma} \\ x^2\dfrac{d^2\tau(x)}{dx^2} + x\dfrac{d\tau(x)}{dx} - x^2\tau(x) = 0 & ; \quad x \ge \dfrac{hka}{\gamma} \end{cases} \tag{A.6}$$

which are recognized as homogeneous and inhomogeneous modified Bessel equations. The general solution of the second equation in A.6 is $\tau(x) = C \cdot I_0(x) + D \cdot K_0(x)$, where $I_0(x)$ and $K_0(x)$ zero order are modified Bessel functions of the first and second kind, respectively. The general solution of the first equation in (A.6) is likewise given by

$g(x) = E \cdot I_0(x) + F \cdot K_0(x) + \frac{1}{A}\left(\frac{\gamma}{hk}\right)^2$. Since the potential must be non-singular both at $x = 0$ and at $x \to \infty$, one must have $F = C = 0$. Moreover, two connection relations must be guaranteed at the outer edge $r = a$ of the space charge density distribution, *i.e.* a continuity of the potential $f(z')g(X) = \sigma(z')\tau(X) \quad \forall \; z'$, and the radial electric field $f(z')\frac{dg(x = X)}{dx} = \sigma(z')\frac{d\tau(x = X)}{dx} \quad \forall \; z'$, where $X = \frac{ka}{\gamma}$. These conditions are equivalent to:

$$A\frac{4\pi\rho_0 b_h}{\gamma}\left[E \cdot I_0(hX) + \frac{1}{A}\left(\frac{\gamma}{hk}\right)^2\right] = B \cdot D \cdot K_0(hX) \tag{A.7}$$

and

$$A\frac{\rho_0 b_h}{\pi\varepsilon_0\gamma}E \cdot I_1(hX) = -B \cdot D \cdot K_1(hX) \tag{A.8}$$

The solutions for the integration constants, namely A, B, D and E, are $A = B = 1$, and, using the Wronskian relation for the modified Bessel functions,

$$D = \frac{4\pi\rho_0 b_h}{\gamma}\frac{(\gamma/hk)^2 I_1(hX)}{I_1(hX)K_0(hX) + I_0(hX)K_1(hX)} = \frac{4\pi\rho_0 b_h\gamma}{hk^2}X \cdot I_1(hX) \tag{A.9}$$

and $$E = \frac{-(\gamma/hk)^2 K_1(hX)}{I_1(hX)K_0(hX) + I_0(hX)K_1(hX)} = -(\gamma/hk)^2 hX \cdot K_1(hX). \tag{A.10}$$

Finally, the expression of the electrostatic potential $\varphi_h(r, z')$ in the beam rest frame is:

$$\begin{cases} \varphi_h(r,z') = \frac{4\pi\rho_0 b_h\gamma}{h^2k^2}\cos\left(h\frac{k}{\gamma}z' + \theta_h\right)\left[1 - hX \cdot K_1(hX)I_0(\frac{hk}{\gamma}r)\right] & ; \quad 0 \le r \le a \\ \varphi_h(r,z') = \frac{4\pi\rho_0 b_h\gamma}{h^2k^2}\cos\left(h\frac{k}{\gamma}z' + \theta_h\right)hX \cdot I_1(hX)K_0(\frac{hk}{\gamma}r) & ; \quad r \ge a \end{cases} \tag{A.11}$$

We are interested in the axial electric field, which is responsible for the space charge oscillations described in this paper; this can be easily calculated, in the rest frame, by $E_z^{rest}(r,z') = -\partial\varphi/\partial z'$, to obtain

$$\begin{cases} E_z^{rest} = \dfrac{4\pi\rho_0}{k}\sum\limits_{h=1}^{\infty}\left\{\dfrac{b_h}{h}\sin\left(h\dfrac{k}{\gamma}z'+\theta_h\right)\left[1-hX\cdot K_1(hX)I_0(\dfrac{hk}{\gamma}r)\right]\right\} \; ; \quad 0\le r\le a \\ E_z^{rest} = \dfrac{4\pi\rho_0}{k}\sum\limits_{h=1}^{\infty}\left\{\dfrac{b_h}{h}\sin\left(h\dfrac{k}{\gamma}z'+\theta_h\right)hX\cdot I_1(hX)K_0(\dfrac{hk}{\gamma}r)\right\} \quad ; \quad r\ge a \end{cases} \tag{A.12}$$

The field transformation back to the laboratory frame is straightforward, being $E_z^{lab}(r,\phi_h) = E_z^{rest}(r,z'=z\gamma)$, hence

$$\begin{cases} E_z^{lab} = \dfrac{4\pi\rho_0}{k}\sum\limits_{h=1}^{\infty}\left\{\dfrac{b_h}{h}\sin(\phi_h)\left[1-hX\cdot K_1(hX)I_0(\dfrac{hk}{\gamma}r)\right]\right\} \; ; \quad 0\le r\le a \\ E_z^{lab} = \dfrac{4\pi\rho_0}{k}\sum\limits_{h=1}^{\infty}\left\{\dfrac{b_h}{h}\sin(\phi_h)hX\cdot I_1(hX)K_0(\dfrac{hk}{\gamma}r)\right\} \quad ; \quad r\ge a \end{cases} \tag{A.13}$$

The on-axis field, $E_{AX}(\phi_h) \equiv E_z^{lab}(r=0,\phi_h)$, is

$$E_{AX} = \frac{4\pi\rho_0}{k}\sum_{h=1}^{\infty}\frac{b_h}{h}\sin(\phi_h)\left[1-hX\cdot K_1(hX)\right]. \tag{A.14}$$

It is interesting to calculate, for completeness, the transverse electric field, using $E_r^{rest}(r,z') = -\partial\varphi/\partial r$ and $E_r^{lab}(r,\phi_h) = \gamma E_r^{rest}(r,z'=z\gamma)$. We find

$$\begin{cases} E_r^{lab} = \dfrac{4\pi\rho_0}{k}\gamma\sum\limits_{h=1}^{\infty}\dfrac{b_h}{h}\cos(\phi_h)hX\cdot K_1(hX)I_1(\dfrac{hk}{\gamma}r) \quad ; \quad 0\le r\le R \\ E_r^{lab} = \dfrac{4\pi\rho_0}{k}\gamma\sum\limits_{h=1}^{\infty}\dfrac{b_h}{h}\cos(\phi_h)hX\cdot I_1(hX)K_1(\dfrac{hk}{\gamma}r) \quad ; \quad r\ge R \end{cases} \tag{A.15}$$

which gives, to lowest order in r

$$E_r^{lab} = 2\pi\rho_0 r \sum_{h=1}^{\infty} b_h \cos(\phi_h)(hX)K_1(hX). \qquad \text{(A.16)}$$

The radial field is proportional to the quantity $hX \cdot K_1(hX)$, the identical normalized factor by which the longitudinal is degraded due to 2-D effects.

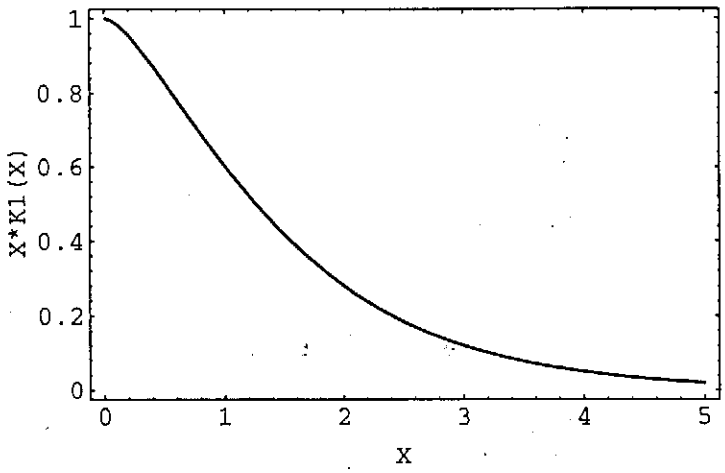

Fig. A.1: Plot of the function $X \cdot K_1(X)$.